Novel Technetium (III)-Q Complexes for Functional Imaging of Multidrug Resistance (*MDR1*) P-Glycoprotein

Carolyn L. Crankshaw, Mary Marmion, Gary D. Luker, Vallabhaneni Rao, Julie Dahlheimer, B. Daniel Burleigh, Elizabeth Webb, Karen F. Deutsch and David Piwnica-Worms

Laboratory of Molecular Radiopharmacology, Mallinckrodt Institute of Radiology, and Department of Molecular Biology and Pharmacology, Washington University Medical School; and Mallinckrodt Medical Group, St. Louis, Missouri

Overexpression of the multidrug resistance (*MDR1*) P-glycoprotein (Pgp) correlates with cancer chemotherapeutic failure. Lipophilic cationic radiopharmaceuticals such as ^{99m}Tc-sestamibi, ^{99m}Tc-tetrofosmin and ^{99m}Tc-furifosmin (Tc-Q12) have been validated as transport substrates for the *MDR1* Pgp and may enable functional imaging of the MDR phenotype in cancer by observing enhanced washout rates of the tracers in those tumor areas expressing Pgp. To further explore and optimize the Pgp recognition properties of Schiff base phosphine mixed-ligand complexes of the Tc-Q series of nonreducible (Tc(III) cations, a variety of Tc-Q complexes were synthesized and tested in vitro for recognition as transport substrates by the human *MDR1* Pgp. **Methods:** Tracer assays with human drug-sensitive KB-3-1 epidermal carcinoma and MDR KB-8-5 cells expressing nonimmunodetectable and modest levels of *MDR1* Pgp, respectively, were used to screen and pharmacologically characterize 37 novel ^{99m}Tc-Q analogs. **Results:** The ideal agent should have low nonspecific binding, high distinction in net uptake between drug-sensitive cells and MDR tumor cells, and high enhancement of uptake in resistant cells after treatment with an MDR modulator, indicating selective blockade of Pgp-mediated efflux of the radiotracer. Three analogs, trans-[5,5′-(1,2-ethanediyldiimino) bis(2-OEt-2-Me-4-penten-3-one)]bis[dimethyl(3-OMe-1-propyl) phosphine]^{99m}Tc(III) (^{99m}Tc-Q63) and two trans-[bis(methyl-bis(3-OMe-1-propyl)phosphine)] analogs (^{99m}Tc-Q57 and ^{99m}Tc-Q58) displayed transport distinctions between drug-sensitive and MDR cell lines that were equal to or greater than all previously available agents. Cyclosporin A, an MDR modulator, had no significant effect in KB-3-1 cells for these ^{99m}Tc-complexes but enhanced tracer accumulations in KB-8-5 cells with IC_{50} values of ~1 μM. In contrast, the non-MDR agents methotrexate and cisplatin had no effect on accumulation of ^{99m}Tc-Q complexes and ^{99m}Tc-sestamibi in KB-8-5 cells. **Conclusion:** Technetium-99m-Q57, ^{99m}Tc-Q58 and ^{99m}Tc-Q63 are avid transport substrates recognized by the human *MDR1* Pgp, and have enhanced in vitro properties that may enable functional imaging of Pgp in vivo with improved signal-to-noise ratios and tissue contrast compared to currently available agents.

Key Words: multidrug resistance; P-glycoprotein; technetium-99m; metal complexes; cyclosporin A

J Nucl Med 1998; 39:77–86

Resistance of malignant tumors to chemotherapy is a major cause of treatment failure (*1*). Tumors that are initially sensitive to cytotoxic agents often become refractory to multiple chemotherapeutic drugs. Cells or tissues obtained from tumors and grown in the presence of a selecting cytotoxic drug can develop cross-resistance to other drugs in that class, as well as other classes of drugs, including anthracyclines, epipodophyllotoxins, paclitaxel and the *Vinca* alkaloids (*1*). The best-characterized mechanism of this multidrug resistance (MDR) phenotype in tumors is increased expression of a M_r 170,000 transmembrane glycoprotein, P-glycoprotein (Pgp), the product of the *MDR1* gene (*2,3*). Transfection of cloned *MDR1* is sufficient to cause MDR in experimental systems (*2*). Thus, acquired resistance to a single drug results in resistance to a diverse group of drugs that are structurally and functionally unrelated but tend to be lipophilic and monocationic at physiological pH values.

P-glycoprotein appears to function as an energy-dependent efflux pump for reducing intracellular concentrations of many natural-product chemotherapeutic agents. By transporting cytotoxic agents out of cells, Pgp is thought to render tumors resistant to chemotherapy. Reversal of MDR by nontoxic agents (known as MDR modulators) that block the transport activity of Pgp has been an important target of pharmaceutical development (*4–6*). In addition, in many different tumors, expression of Pgp and related transporters (e.g., the MDR-associated protein) (*7*) are important prognostic indicators. Increased levels of *MDR1* Pgp and MDR-associated protein have been found in tumor biopsies from cancer patients with poor clinical outcomes (*8,9*). A noninvasive method to functionally detect MDR in tumors would be an important diagnostic assay for management and prognostic stratification of cancer patients.

Technetium-99m-sestamibi, ^{99m}Tc-tetrofosmin and ^{99m}Tc-furifosmin (Tc-Q12-complex) are lipophilic cationic radiotracers that were originally designed for imaging myocardial perfusion (*10–12*). They recently have been validated as transport substrates for Pgp in a variety of multidrug-resistant human and rodent cells (*13–19*). Net cellular accumulation of the tracers is inversely proportional to the level of Pgp expression, and enhancement of radiotracer content is observed after exposure to MDR modulators. In rodent models, faster clearance of ^{99m}Tc-sestamibi is observed in tumors that express Pgp, as compared with malignancies that do not express the MDR gene product (*13,15*). Scintigraphic data in patients with breast cancer demonstrate that ^{99m}Tc-sestamibi washout rates from breast cancers overexpressing *MDR1* Pgp are threefold faster than those from cancers not expressing elevated levels of the transporter (*20*). In addition, clinically relevant levels of a high-potency MDR modular, Novartis PSC 833, block *MDR1* Pgp-mediated clearance of ^{99m}Tc-sestamibi from the liver and kidney (*21*).

To further explore and optimize the *MDR1* Pgp recognition properties of the Tc-Q series of nonreducible Tc(III) cations, a variety of novel Tc-Q complexes were synthesized and tested for recognition as transport substrates by the human *MDR1* Pgp. Technetium-Q complexes are a class of cationic mixed ligand Tc(III) complexes containing both a Schiff base and two monodentate phosphine ligands in an octahedral coordination

Received Nov. 25, 1996; revision accepted Mar. 24, 1997.

For correspondence or reprints contact: David Piwnica-Worms, MD, PhD, Mallinckrodt Institute of Radiology, Washington University Medical School, Campus Box 8225, 510 South Kingshighway Blvd., St. Louis, MO 63110.

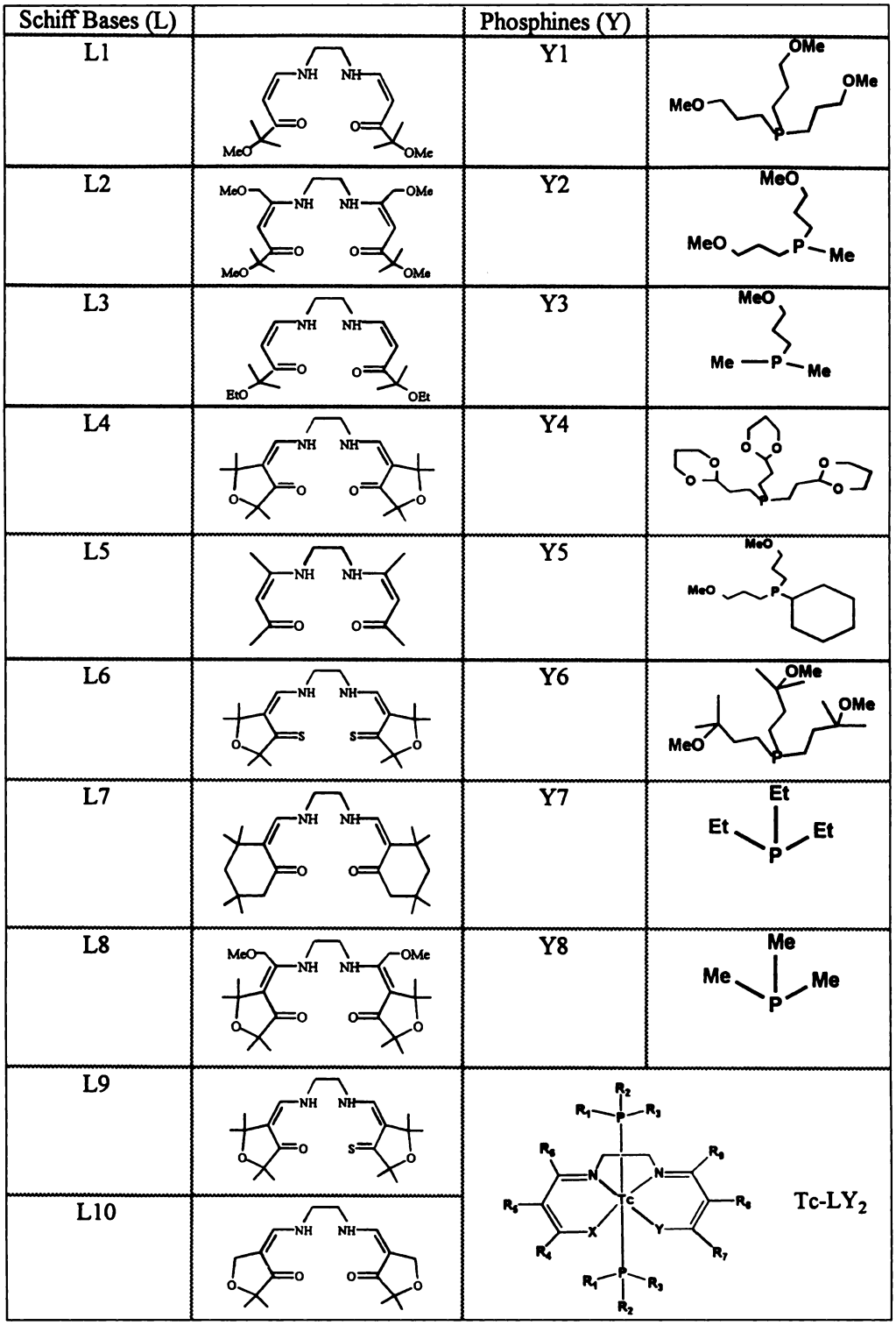

FIGURE 1. Structure of tetradentate Schiff base ligands (L) and monodentate phosphine ligands (Y) used to generate the ^{99m}Tc-L(Y)$_2$ complexes (Tc-Q complexes) screened for *MDR1* Pgp transport activity. Code names for each Tc(III)-Q complex derived from various combinations of these ligands are shown in Table 1. General structure of a Tc-Q complex is shown in the lower right corner (where small x and y represent either O or S).

geometry around the central metal. The broad drug-binding and transport properties of Pgp suggest that selected ^{99m}Tc-Q compounds could be designed to mimic known MDR agents. The lipophilicity and Pgp-targeting properties of these complexes can be readily adjusted by varying functionalities on the Schiff base or phosphine moieties independently (Fig. 1). Hence, this approach allows the coordination environment of the Tc(III) metal core to be maintained while the overall electronic environment is altered, thereby enabling refined exploration and evaluation of Pgp-mediated transport properties.

Using a targeted medicinal chemistry approach, the goal of this project was to design, synthesize and quantitatively optimize novel ^{99m}Tc-Q complexes as transport substrates of the human *MDR1* Pgp. Human KB-3-1 epidermal carcinoma and the derivative multidrug-resistant KB-8-5 cells were used to selectively screen the 37 Tc-Q complexes. A series of Pgp transport indices was developed to assist our analysis and characterization. This took into account pharmacological and experimental criteria that desirable *MDR1* targeted Tc-Q complexes would have the following properties:

1. Low nonspecific binding to cells, membranes and hydrophobic regions in biological preparations;

2. High distinction in net uptake levels between drug-sensitive cells and Pgp-expressing MDR cells; and
3. High enhancement of uptake in resistant cells on addition of a classic MDR modulator, in this case, cyclosporin A (the "modulator-challenge test").

The sum of the ratios of various experimentally determined values allowed calculation of an MDR selectivity index (SI) to rank those Tc-Q complexes with the most desirable properties in vitro. Data for ^{99m}Tc-sestamibi and ^{99m}Tc-tetrofosmin under identical conditions were generated for comparison. Three analogs, the trans-[5,5'-(1,2-ethanediyldiimino)bis(2-OEt-2-Me - 4 - penten - 3 - one)]bis[dimethyl(3-OMe-1-propyl)phosphine] Tc(III) (Tc-Q63) and two trans-[bis(methyl-bis(3-OMe-1-propyl)phosphine)] analogs (Tc-Q57 and Tc-Q58), displayed distinctions between nonexpressing and *MDR1* Pgp-expressing cell lines that were greater than those of all previously available agents and, thus, are candidates for further clinical development.

MATERIALS AND METHODS

Preparation of Technetium-99m-Q Complexes

Synthesis of the radiolabeled ^{99m}Tc-Q complexes was performed by minor modification of general methods described previously (*12,22,23*). A standard two-step procedure was used as follows. In the first step, $^{99m}TcO_4^-$, from a commercial generator (50–100 mCi, 1 ml), was added to a vial containing 10–15 mg of the Schiff base ligand in 0.1 ml ethanol. The solution was deaerated for 15 min with a vigorous stream of argon or nitrogen; 15 mg $SnCl_2$ (in degassed ethanol), and 0.03 ml of 1 *M* NaOH then were added. The preparation was subsequently incubated for 10 min at 75°C to yield the ^{99m}Tc(V) intermediate. In the second step, 2.5 mg of the phosphine ligand (10 mg/ml ethanol/0.1 *N* HCl) were added to the warm ^{99m}Tc(V) preparation, and the resulting solution was heated for 10 min at 75°C to yield the desired ^{99m}Tc-Q complex. Separation of the radiolabeled complex from impurities and reaction reagents was performed by high-performance liquid chromatography (HPLC) purification using a reverse-phase PRP-1 column (250 × 4.1 mm, 10 μm) and an acetonitrile (pH 5.3):5 m*M* KH_2PO_4 (pH 6.7) gradient. The HPLC eluent then was removed from the desired complex by diluting the collected HPLC fraction with water, loading it onto a prewetted C18 Sep-Pak and eluting the product with ethanol:saline (80:20). The eluate was diluted with normal saline to obtain an ethanol concentration of 10%. Quality control, effected by reverse-phase HPLC (same conditions as above), showed >90% radiochemical purities.

All synthesized ^{99m}Tc-Q complexes are identified and characterized in Figure 1 and Table 1. Retention times for all agents were determined by HPLC using a PRP-1 column (250 × 4.1 mm; 10 μm) and an acetonitrile:5 m*M* KH_2PO_4 gradient (20%–80% in 20 min) at a flow rate of 2.0 ml/min. Selected preparation of the most biologically favorable compounds are described below.

Technetium-99m-Q12 {trans-[1,2-bis(dihydro-2,2,5,5-tetramethyl-3(2H)furanone - methyleneimino)ethane]bis[tris(3-methoxy-1-propyl) phosphine]technetium(III)}$^+$. The synthesis of this complex has been previously reported (*12*).

Technetium-99m-Q57 {trans-[5,5' - (1,2 - ethanediyldiimino)bis(2 - ethoxy-2-methyl-4-penten-3-one)]bis[methyl-bis(3-methoxypropyl)phosphine]technetium(III)}$^+$. In the first step, $^{99m}TcO_4^-$ from a commercial generator (50–100 mCi, 1 ml) was added to a vial containing 15 mg of 5,5'-(1,2-ethanediyldiamino)bis(2-ethoxy-2-methyl-4-penten-3-one) in 0.1 ml ethanol. The solution was deaerated for 15 min with a vigorous stream of argon; 15 μg $SnCl_2$ (in degassed ethanol), and 0.03 ml of 1 *M* NaOH were then added. The preparation was subsequently incubated for 10 min at 75°C to yield the ^{99m}Tc(V) intermediate. In the second step, 2.5 mg of a methyl-bis(3-methoxypropyl)phosphine (10 mg/ml ethanol/0.1 *N* HCl) were added to the ^{99m}Tc(V) preparation, and the solution was heated for 10 min at 75°C to yield the desired ^{99m}Tc-Q57 complex. Separation of the radiolabeled complex from reagents was performed by HPLC purification using a reverse-phase PRP-1 column (250 × 4.1 mm, 10 μm) and an acetonitrile:5 m*M* KH_2PO_4 gradient. Quality control, effected by reverse-phase HPLC (same conditions as above), showed 98% radiochemical purity (retention time = 14.7 min).

Technetium-99m-Q58 {trans-[2,2'-(1,2-ethanediyldiimino)bis(1,5-dimethoxy-5-methyl-2-hexen-4-one)]bis[methyl-bis(3-methoxypropyl) phosphine]technetium(III)}$^+$. In the first step, $^{99m}TcO_4^-$ from a commercial generator (50–100 mCi, 1 ml) was added to a vial containing 15 mg of 2,2'-(1,2-ethanediyldiamino)bis(1,5-dimethoxy-5-methyl-2-hexen-4-one) in 0.1 ml ethanol. The solution was deaerated for 15 min with a vigorous stream of argon; 15

TABLE 1
Nomenclature and Acryonyms of Novel Technetium-99m-Q Complexes*

Q no.	Formula [^{99m}Tc-L(Y)$_2$]	Plasma binding (%)	HPLC retention time (min)
Q3	^{99m}Tc-L5(Y1)$_2$	4	14.7
Q5	^{99m}Tc-L5(Y4)$_2$	5	17.1
Q6	^{99m}Tc-L1(Y1)$_2$		13.7
Q11	^{99m}Tc-L2(Y1)$_2$		16.1
Q12	^{99m}Tc-L4(Y1)$_2$	2	14.7
Q15	^{99m}Tc-L5(Y6)$_2$		20.4
Q16	^{99m}Tc-L3(Y1)$_2$		15.8
Q17	^{99m}Tc-L6(Y1)$_2$		15.3
Q18	^{99m}Tc-L4(Y2)$_2$	2	12.8
Q19	^{99m}Tc-L9(Y1)$_2$		14.3
Q25	^{99m}Tc-L4(Y4)$_2$		16.4
Q26	^{99m}Tc-L10(Y1)$_2$		12.9
Q28	^{99m}Tc-L4(Y3)$_2$	2	12.3
Q40	^{99m}Tc-L4(Y7)$_2$	50	17.8
Q41	^{99m}Tc-L7(Y1)$_2$		23.3
Q43	^{99m}Tc-L8(Y1)$_2$		17.8
Q44	^{99m}Tc-L10(Y5)$_2$		19.4
Q45	^{99m}Tc-L4(Y6)$_2$		20.9
Q46	^{99m}Tc-L4(Y8)$_2$	2	12.6
Q47	^{99m}Tc-L10(Y4)$_2$		14.0
Q48	^{99m}Tc-L10(Y6)$_2$		18.7
Q49	^{99m}Tc-L10(Y7)$_2$		14.0
Q50	^{99m}Tc-L10(Y8)$_2$		9.0
Q51	^{99m}Tc-L3(Y8)$_2$	100	13.4
Q52	^{99m}Tc-L1(Y4)$_2$		16.0
Q53	^{99m}Tc-L2(Y4)$_2$		16.0
Q54	^{99m}Tc-L1(Y8)$_2$		12.7
Q55	^{99m}Tc-L2(Y8)$_2$	14	13.4
Q56	^{99m}Tc-L1(Y2)$_2$		12.6
Q57	^{99m}Tc-L3(Y2)$_2$	2	14.5
Q58	^{99m}Tc-L2(Y2)$_2$	1	13.9
Q59	^{99m}Tc-L5(Y2)$_2$		13.4
Q60	^{99m}Tc-L10(Y2)$_2$	2	10.6
Q61	^{99m}Tc-L2(Y3)$_2$	3	13.6
Q62	^{99m}Tc-L1(Y3)$_2$	2	12.6
Q63	^{99m}Tc-L3(Y3)$_2$	4	15.5
Q64	^{99m}Tc-L5(Y3)$_2$		13.0

*The formula that indicates the Schiff base/phosphine ligand combination used to generate each Tc-Q complex refers to the structures identified in Figure 1. Also shown for each Tc-Q complex is the corresponding HPLC retention time (minutes) and, for several complexes, the corresponding human plasma binding (% of total activity).

μg $SnCl_2$ (in degassed ethanol), and 0.03 ml of 1 *M* NaOH were then added. The preparation subsequently was incubated for 10 min at 70°C to yield the ^{99m}Tc(V) intermediate. In the second step, 2.5 mg of a methyl-bis(3-methoxypropyl)phosphine (10 mg/ml ethanol/0.1 *N* HCl) were added to the ^{99m}Tc(V) preparation, and the solution was heated for 10 min at 70°C to yield the desired ^{99m}Tc-Q58 complex. Separation of the radiolabeled complex from reagents was performed by HPLC purification using a reverse-phase PRP-1 column (250 × 4.1 mm, 10 μm) and an acetonitrile:5 m*M* KH_2PO_4 gradient. Quality control, effected by reverse-phase HPLC (same conditions as above), showed 96% radiochemical purity (retention time = 13.9 min).

Technetium-99m-Q63, {trans-[5,5'-(1,2-ethanediyldiimino)bis(2-ethoxy-2-methyl-4-penten-3-one)]bis[dimethyl(3-methoxypropyl) phosphine]technetium(III)}$^+$. In the first step, $^{99m}TcO_4^-$ from a commercial generator (50–100 mCi, 1 ml) was added to a vial containing 15 mg of 5,5'-(1,2-ethanediyldiamino)bis(2-ethoxy-2-methyl-4-penten-3-one) in 0.1 ml ethanol. The solution was deaerated for 15 min with a vigorous stream of argon; 15 μg $SnCl_2$ (in degassed ethanol), and 0.03 ml of 1 *M* NaOH were then added. The preparation was subsequently incubated for 10 min at 75°C to yield the ^{99m}Tc(V) intermediate. In the second step, 2.5 mg of a dimethyl(3-methoxypropyl)phosphine (10 mg/ml ethanol/0.1 *N* HCl) were added to the ^{99m}Tc(V) preparation, and the solution was heated for 10 min at 75°C to yield the desired ^{99m}Tc-Q63 complex. Separation of the radiolabeled complex from reagents was performed by HPLC purification using a reverse-phase PRP-1 column (250 × 4.1 mm, 10 μm) and an acetonitrile:5 m*M* KH_2PO_4 gradient. Quality control, effected by reverse-phase HPLC (same conditions as above), showed 96% radiochemical purity (retention time = 15.5 min).

Synthesis of Schiff Bases: General

Ether functionality can be incorporated into the equatorial Schiff base ligand by condensation of diamines with ether-containing β-dicarbonyl compounds (*24*). The presence of the aldehyde moiety and *gem*-dimethyl groups allow for a straightforward high-yielding synthesis. The synthetic scheme of the key Schiff base ligands are as follows:

Scheme 1

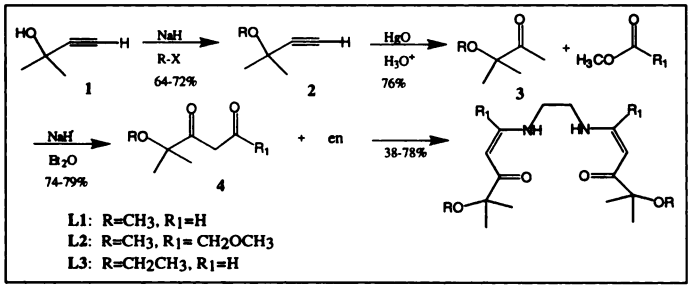

Three ethylenediamine(acetylacetone)$_2$ derivatives that incorporate the tertiary ether moiety were synthesized, starting from the mono adduct of acetylene and acetone. Alkylation of 2-methyl-3-butyn-2-ol (**1**) provided the tertiary methyl and ethyl ethers **2** (R = CH_3, CH_2CH_3). Mercury-assisted hydrolysis of the triple bond gave the methyl ketones **3**. The presence of α-dimethyl groups prevents deprotonation at the α-alkoxy carbon. This results in clean anion formation at the less hindered side of the ketone during the Claisen condensation step. Acylation with ethyl formate is clean and high yielding. Lower yields of **4** (R = CH_3, R_1 = CH_2OCH_3) were obtained with ethyl methoxyacetate because of competing Claisen condensations. Reaction of the β-dicarbonyl tertiary ethers with ethylenediamine provided the crystalline Schiff base ligands, **L1**, **L2** and **L3**. The α-*gem*-dimethyl groups also hinder the attack of the diamine at the adjacent ketone. This results in regioselective condensation at the less hindered carbonyl. Details for specific synthesis and analytical characterization of desired Schiff base ligands (**L**) and intermediates are further described in supplementary material posted on the World Wide Web (http://www.imaging.wustl.edu/molec-pharm/piwnica-worms).

Synthesis of Phosphine Ligands: General

Preparation of the tertiary phosphines was accomplished in a two-step, one-pot reaction, according to the reaction described below, with an overall yield of 50%–70%:

Scheme 2

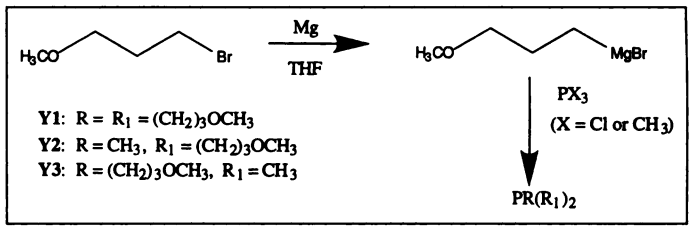

To ground Mg (100 mmol) in tetrahydrofuran (THF) (25 ml) was added one crystal of I_2 and one drop of 1,2-dibromoethane, followed by several drops of halide (100 mmol) in THF (25 ml), and the reaction was initiated by warming. The remaining halide/THF solution was added at a rate that maintained a gentle reflux. The reflux was continued for 2 hr postaddition, by external heating. The material was diluted with THF (50 ml), cannula-transferred (away from unreacted Mg metal) to a fresh dry flask under argon, cooled to −78°C and stirred for 30 min. PX_3 (15 mmol) in THF (5 ml) was added dropwise over 1 hr, allowed to warm to room temperature gradually and heated to reflux for 2 hr thereafter. The reaction was cooled to 10°C and quenched by dropwise addition of deaerated water (10 ml). The THF solution was cannula-transferred onto 20 g of Na_2SO_4, allowed to dry for 6 hr and cannula-transferred to a fresh flask. The THF was removed by distillation, and the residue was purified by distillation or recrystallization as indicated. Details for specific synthesis and analytical characterization of desired phosphine ligands (**Y**) is further described in supplementary material posted on the World Wide Web (http://www.imaging.wustl.edu/molec-pharm/piwnica-worms).

Plasma Binding

Human plasma binding values of ^{99m}Tc-Q complexes in vitro were determined by Sephadex filtration. Samples (~5 mCi) were analyzed by fast protein liquid chromatography using a Sephadex G-50 gel filtration HR 10/10 (100 × 10 mm) column (Pharmacia) packed with Sephadex G-50 Fine (Pharmacia) and phosphate-buffered saline (PBS) at a flow rate of 1 ml/min. Before analysis, the column was blocked with 1 ml of a 2.5% bovine serum albumin/PBS solution, followed by a PBS flush, to avoid adhesion of plasma proteins to the column. A volume of 0.05 ml of the test agent was mixed with 0.2 ml human plasma and 0.75 ml PBS, incubated in a 37°C water bath for 30 min, spin-filtered using a 0.45-μm filter for 2 min at 6000 rpm and injected onto the preblocked G-50 column for protein-binding analysis.

Preparation of Technetium-99m-Sestamibi and Technetium-99m-Tetrofosmin

The radiopharmaceuticals ^{99m}Tc-sestamibi (Dupont Radiopharmaceuticals, Billerica, MA) and ^{99m}Tc-tetrofosmin (Amersham, International, Buckinghamshire, UK) were prepared from kit formulations by addition of $^{99m}TcO_4^-$, according to the manufacturers' recommendations. Separation of the radiolabeled ^{99m}Tc-tetrofosmin from kit reagents was accomplished by diluting the preparation with 20 ml water, loading it onto

a prewet C18 Sep-Pak and eluting the product with ethanol: saline (80:20). The eluate was diluted with normal saline to obtain an ethanol concentration of 10%. Purification of ^{99m}Tc-sestamibi was performed as described previously (*25*). Quality control, effected by reverse-phase HPLC (same conditions as above), showed > 95% radiochemical purities.

Cells and Solutions

Human drug-sensitive KB-3-1 epidermal carcinoma cells and the colchicine-selected KB-8-5 derivative cell lines were grown as described (*3,26*). Briefly, cells were plated in 100-mm Petri dishes containing seven 25-mm glass coverslips on the bottom and grown to confluence in Dulbecco's modified Eagle's medium (GIBCO, Grand Island, NY) supplemented with L-glutamine (2 m*M*), 0.1% penicillin/streptomycin and 10% heat-inactivated fetal calf serum in the absence or presence of 10 ng/ml colchicine, respectively.

Control solution for transport experiments was a modified Earle's balanced salt solution (MEBSS) containing: 145 m*M* Na^+, 5.4 m*M* K^+, 1.2 m*M* Ca^{2+}, 0.8 m*M* Mg^{2+}, 152 m*M* Cl^-, 0.8 m*M* $H_2PO_4^-$, 0.8 m*M* SO_4^{2-}, 5.6 m*M* dextrose, 4.0 m*M* HEPES and 1% bovine calf serum (vol/vol), pH 7.4 ± 0.05. A 130 m*M* K/19 m*M* Cl solution was made by equimolar substitution of K-methanesulfonate for NaCl, as described (*27*). Valinomycin (Sigma Chemical Co., St. Louis, Mo.) was dissolved in dimethylsulfoxide before being added to solutions, and cyclosporin A (Novartis Pharmaceuticals, cremophor formulation) was added directly to buffers. Final vehicle concentration was typically <0.1%, a level found to have no effect on net uptake of ^{99m}Tc tracers in cultured cells (*25*).

Cell Tracer Studies

Coverslips with confluent cells were removed from culture medium and preequilibrated for 20–30 sec in control buffer. Uptake and retention experiments were initiated by immersion of coverslips in 60-mm glass Pyrex dishes containing 4 ml loading solution, consisting of MEBSS with 0.1–0.6 nM_o radiolabeled Tc-Q complex (5–9 pmol/mCi; 1–3 μCi/ml). Cells on coverslips were removed at the indicated times, rinsed three times in 25 ml ice-cold (4°C) isotope-free MEBSS solution for 8 sec each to clear extracellular spaces and placed in 35-mm plastic Petri dishes. Cells were extracted in 1% sodium dodecylsulfate with 10 m*M* Na-borate for at least 30 min before aliquots were obtained for gamma counting and protein assay by the method of Lowry, using bovine serum albumin as the protein standard. Aliquots of the loading buffer and standard solutions also were obtained for normalizing cellular data to the extracellular concentration (nM_o) of novel Tc-Q complexes. Cell extracts, standard solutions and extracellular buffer samples were assayed for gamma activity in a well scintillation sodium iodide gamma counter (Minaxi 5500; Packard, Meridan, CT). Knowledge of the elution history of the Mo/Tc generators (Mallinckrodt, Inc.) and activity of stock solutions allowed the use of generator equilibrium equations (*28*) to calculate the absolute concentration of total Tc-Q complex in each buffer as described (*17*). Note that data are ultimately presented as fmol/(mg protein·nM_o), which is essentially an in-to-out ratio of tracer content and, therefore, independent of counting efficiency and generator elution history.

Western Blots

P-glycoprotein content was determined in enriched membrane preparations from drug-sensitive and multidrug-resistant cells by Western blotting, using mouse anti-Pgp monoclonal antibody (MAb) C219 (Signet Corp., Dedham, MA). Immune complexes were revealed with goat anti-mouse antibody coupled to alkaline phosphatase as described (*14*). Cell cultures were randomly checked at bimonthly intervals for Pgp expression with no significant change identified over the course of the study.

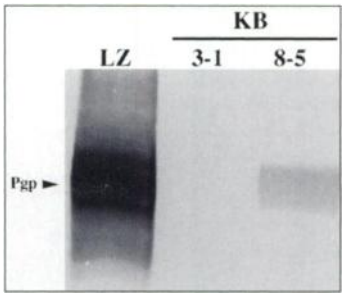

FIGURE 2. Expression of *MDR1* Pgp in human KB-3-1 and KB-8-5 epidermal carcinoma cells, as determined by Western blots of plasma membrane preparations with MAb C219. Membranes from highly MDR hamster LZ-8 cells are shown for comparison. Arrow, 170 kDa.

Statistical Analysis

All data points were determined in quadruplicate from preparations obtained from the same culture. Multiple comparisons were made by one-way analysis of variance (*29*). Pairs were compared by the Student's t-test. Values of $p < 0.05$ were considered significant.

RESULTS

Chemistry

The Q complexes were prepared in two steps. The first step involved heating pertechnetate in the presence of both the Schiff base ligand (**L**) and a reducing agent, such as stannous chloride, to form a Tc(V) intermediate, and the second step involved the reductive addition of the phosphine ligand (**Y**) to this Tc(V) intermediate to form the desired Tc(III) agent.

Scheme 3

Step 1: $[^{99m}TcO_4]^- + \mathbf{L} + Sn^{2+} \rightarrow [^{99m}Tc(V)(O)(\mathbf{L})]^+$

Step 2: $[^{99m}Tc(V)(O)(\mathbf{L})]^+ + 2\mathbf{Y} \rightarrow [^{99m}Tc(III)(\mathbf{L})(\mathbf{Y})_2]^+$

In most cases, purification by HPLC was required to obtain radiochemical purities of >90%. Selected Tc(III) cations have been characterized by fast atom bombardment–mass spectrometry (FAB-MS) (using "carrier" ^{99}Tc), and retention times (Table 1) of all Tc(III)-Q cations were consistent with the proposed structures.

Cell Tracer Assays

Human drug-sensitive KB-3-1 epidermal carcinoma cells and the colchicine-selected MDR KB-8-5 derivative cell line were chosen for use in analysis of the Pgp-targeted transport properties of ^{99m}Tc-Q complexes. Western blots of crude cell membrane preparations with the anti-Pgp mAb C219 showed no immunodetectable *MDR1* Pgp in KB-3-1 cells and modest levels of Pgp in the KB-8-5 cells (Fig. 2). Shown for comparison are LZ-8 cells, a highly multidrug-resistant hamster lung fibroblast line (*17*), which displayed much higher levels of Pgp, supporting the premise that the KB-8-5 cells expressed a clinically relevant, modest level of wild-type human *MDR1* Pgp (*30*).

To validate the drug screening protocol, ^{99m}Tc-sestamibi, an established probe of *MDR1* Pgp transport function (*17,18*) was used to characterize tracer uptake and reversal in the human cell lines expressing the different levels of Pgp. Technetium-99m-sestamibi was accumulated by each cell line to a plateau within 30 min, and steady-state levels of the radiolabel could be maintained for up to 2 hr. Plateau levels of ^{99m}Tc-sestamibi in the cell lines were inversely related to the expression of Pgp (Fig. 3A), consistent with enhanced cellular extrusion of the imaging agent by the transporter. In KB-3-1 cells, steady-state uptake (30 min) of ^{99m}Tc-sestamibi was 187 ± 12 fmol/(mg

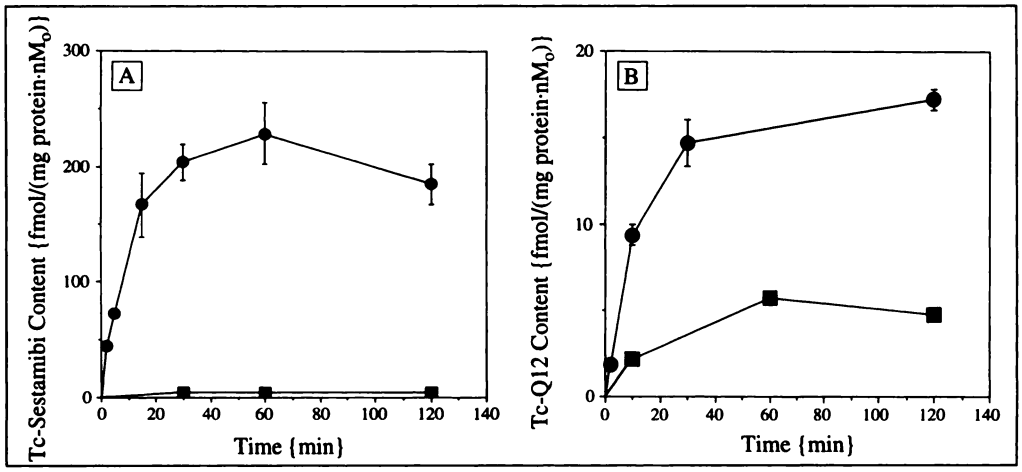

FIGURE 3. Kinetics of ^{99m}Tc-sestamibi (A) and Tc-Q12 (B) accumulation in KB-3-1 cells (●) and MDR KB-8-5 (■) cells. Each point represents the mean value ± s.e.m. of four determinations.

protein·nM_o) (mean ± s.e.m.; n = 4), whereas in KB-8-5 cells, net uptake was 3.9 ± 0.2 (Table 2).

On addition of a MDR-modulating agent, one desirable property of an ideal *MDR1* Pgp transport assay would be full reversal (enhancement) of net tracer accumulation in KB-8-5 cells to the levels found in drug-sensitive KB-3-1 cells but no effect on addition to the KB-3-1 cells. Addition of cyclosporin A, a classic MDR modulator (*4*), enhanced accumulation of ^{99m}Tc-sestamibi to 179 ± 6.0 fmol/(mg protein·nM_o) in KB-8-5 cells (Fig. 4A) and caused a 46-fold increase in ^{99m}Tc-sestamibi content but produced only a 1.5-fold increase in KB-3-1 cells, a value that could not be attributed to inhibition of Pgp function. The IC_{50} of reversal in KB-8-5 cells was 1.5 μg/ml (1.2 μ*M*) and maximal reversal occurred by 6 μg/ml (5 μ*M*); therefore, Tc-Q complexes were screened for reversal at this saturating concentration.

Another desirable property of lipophilic cations that may enhance net tissue accumulation in vivo is the ability to rapidly respond to the negative transmembrane potentials generated in living cells by concentrating within the cytoplasm and mitochondrial matrix of non-Pgp-expressing cells (*13,25*). Incubation of KB-3-1 cells in 130 m*M* K buffer, containing the ionophore valinomycin (1 μg/ml), depolarizes mitochondrial and plasma membrane potentials toward zero (*25*), and thus, the high K^+/valinomycin-sensitive component is one measure of the ability of the test compound to respond to transmembrane potentials. Conversely, the residual tracer remaining in high K^+/valinomycin buffer measures the nonmembrane potential component of tracer accumulation, one determinate of nonspecific cell binding of the agent. Net uptake of ^{99m}Tc-sestamibi in KB-3-1 cells under high K^+/valinomycin conditions was 5.1 ± 0.1 fmol/(mg protein·nM_o) (Fig. 4A). Typical cell water spaces of transformed cells are in the range of 5.4 μl/mg protein (*31*), and when the residual tracer in high K^+/valinomycin buffer was divided by this cell water space, an in-to-out tracer ratio of 0.94 was obtained. As anticipated by the ideal membrane potential responsiveness of ^{99m}Tc-sestamibi (*32*), this value approximates unity under isoelectric conditions, confirming the validity of these assay conditions for screening novel Tc-Q complexes.

The clinically available agent Tc-Q12 was first tested for *MDR1* Pgp transport recognition by these assays (Figs. 3B and 4B). Like other classes of lipophilic cations, cellular accumulation of Tc-Q12 approached a plateau in KB-3-1 cells that was significantly higher than the level found in KB-8-5 cells, consistent with a Pgp-mediated efflux transport mechanism for Tc-Q12. The KB-3-1/KB-8-5 uptake ratio was 14 for Tc-Q12, significantly less than the ratio of 48 determined for ^{99m}Tc-sestamibi. Tc-Q12 accumulation in KB-3-1 cells incubated in high K^+/valinomycin was reduced by 85%, whereas accumulation in KB-8-5 cells incubated with cyclosporin A (6 μg/ml) was partially reversed (Fig. 4B), overall suggesting modest membrane potential responsiveness and Pgp-targeting properties.

To improve on the Pgp recognition properties of Tc-Q12, a series of 36 additional Tc-Q complexes was synthesized and evaluated for *MDR1* Pgp transport properties in the KB cell model. These were directly compared to the commercial agents ^{99m}Tc-sestamibi, Tc-Q12 and ^{99m}Tc-tetrofosmin under identical conditions. Table 2 shows the KB-3-1 and KB-8-5 cell accumulation data for each complex. Several structure–transport relationships were evident. Membrane potential-independent accumulation in non-MDR KB-3-1 cells correlated with lipophilicity (Fig. 5; $r = 0.512$, $p < 0.005$). Thus, the residual tracer accumulation under these conditions appeared to monitor nonspecific binding of the complexes to hydrophobic domains, likely representing adsorption into lipid compartments of the cells. Conversely, there was no well-defined relationship between control uptakes in KB-3-1 cells and lipophilicity or between the ability of the radiotracers to distinguish drug-sensitive and MDR cells and lipophilicity. No single tested Schiff base or phosphine ligand uniquely conferred *MDR1* Pgp transport recognition properties per se, although several of the mixed ligand complexes showed robust Pgp transport profiles (Tc-Q28, Tc-Q51, Tc-Q55, Tc-Q57, Tc-Q58, Tc-Q61, Tc-Q62 and Tc-Q63). Particular examples with Tc-Q58 and Tc-Q63 are shown in Figure 6. These generally possessed modest lipophilicity as determined by HPLC retention times.

Interestingly, substitution of one or both Schiff base ligand carbonyl oxygens by sulfur (Tc-Q19 and Tc-Q17) completely abrogated any *MDR1* Pgp recognition properties of candidate complexes. For example, going from the Schiff base complex Tc-Q12 to its monosubstituted sulfur analog Tc-Q19 reduced the KB-3-1/KB-8-5 ratio from 14 to 3 (Table 2).

To directly compare and rank the efficacy of the complexes for functional assessment of *MDR1* Pgp transport activity, an in vitro SI was devised. On the basis of an approach pioneered by Katzenellenbogen et al. (*33,34*) for the development of radioligands for estrogen and progesterone receptors, several ratios of the in vitro transport data were devised to assist in organizing functional trends in the datasets (Fig. 7). In KB-3-1 cells, the ratio of tracer accumulation in control buffer divided by accumulation in high K buffer was used to monitor the membrane potential responsiveness of a test radiotracer. The ratio of accumulation in KB-3-1 cells divided by accumulation in KB-8-5 cells was a monitor of the *MDR1* Pgp-mediated transport response. In KB-8-5 cells, the ratio of accumulation in the presence of cyclosporin A (6 μg/ml), divided by accumu-

TABLE 2
Characterization of 30-min Accumulations of a Series of Technetium-99m-Q Complexes, Technetium-99m-Sestamibi and Technetium-99m-Tetrofosmin in Drug-Sensitive and Multidrug Resistant Cells*

Technetium complex	Cell content [fmol/(mg protein·nM_o)] KB-3-1	KB-3-1+ K^+/valinomycin	KB-8-5	KB-8-5+ cyclosporin A
Q3	127 ± 2.9	34.0 ± 1.3	5.9 ± 0.4	78.0 ± 2.5
Q5	27.6 ± 1.5	18.0 ± 1.8	5.8 ± 0.3	17.7 ± 0.9
Q6	15.0 ± 0.6	5.2 ± 0.4	1.9 ± 0.1	12.7 ± 0.4
Q11	32.4 ± 2.3	5.3 ± 0.2	5.7 ± 0.2	83.9 ± 12
Q12	30.6 ± 2.4	4.5 ± 0.1	2.2 ± 0.2	15.6 ± 1.2
Q15	1950 ± 91	85.5 ± 6.0	184 ± 25	2260 ± 420
Q16	76.6 ± 6.8	7.6 ± 0.5	3.6 ± 0.4	51.8 ± 2.0
Q17	128 ± 12	101 ± 8.2	184 ± 15	288 ± 15
Q18	19.1 ± 2.2	5.3 ± 0.3	1.3 ± 0.3	9.4 ± 0.4
Q19	74.4 ± 5.8	26.2 ± 0.5	23.3 ± 0.8	39.2 ± 2.3
Q25	13.8 ± 1.8	2.7 ± 0.2	2.9 ± 0.4	25.0 ± 1.8
Q26	2.9 ± 0.3	1.4 ± 0.1	0.5 ± 0.1	2.2 ± 0.1
Q28	16.2 ± 2.0	3.9 ± 0.3	0.4 ± 0.0	7.5 ± 0.9
Q40	1720 ± 110	353 ± 26	64.0 ± 6.0	1340 ± 39
Q41	540 ± 34	186 ± 15	370 ± 37	690 ± 92
Q43	22.5 ± 0.6	12.6 ± 1.4	4.3 ± 0.1	25.1 ± 1.7
Q44	390 ± 30	78.1 ± 3.9	25.6 ± 1.5	315 ± 2.6
Q45	1170 ± 210	131 ± 10	223 ± 21	2540 ± 280
Q46	12.3 ± 0.7	3.3 ± 0.1	0.9 ± 0.1	4.5 ± 0.2
Q47	4.2 ± 0.2	3.1 ± 0.7	1.9 ± 0.3	2.4 ± 0.1
Q48	325 ± 15	74.4 ± 5.0	26.3 ± 5.3	270 ± 18
Q49	538 ± 26	156 ± 8.7	18.0 ± 1.5	299 ± 14
Q50	4.3 ± 0.2	3.6 ± 0.1	2.0 ± 0.1	3.3 ± 0.1
Q51	475 ± 80	103 ± 13	5.8 ± 0.8	240 ± 11
Q52	37.0 ± 1.5	5.0 ± 0.2	3.0 ± 0.2	18.2 ± 1.0
Q53	36.0 ± 2.3	5.3 ± 0.5	3.6 ± 0.2	33.9 ± 1.0
Q54	40.5 ± 6.1	10.8 ± 1.0	3.2 ± 0.2	33.3 ± 0.7
Q55	159 ± 7.5	44.7 ± 2.9	3.5 ± 1.1	140 ± 9.9
Q56	73.3 ± 5.7	18.5 ± 0.8	3.0 ± 1.2	25.8 ± 1.0
Q57	252 ± 20	26.2 ± 3.1	3.7 ± 1.1	145 ± 7.0
Q58	57.9 ± 4.2	7.3 ± 0.3	0.9 ± 0.2	33.1 ± 0.9
Q59	128 ± 8.7	33.9 ± 1.7	5.0 ± 0.2	75.7 ± 3.7
Q60	6.3 ± 0.6	3.6 ± 0.2	0.5 ± 0.0	2.3 ± 0.1
Q61	82.4 ± 5.3	21.4 ± 1.0	2.4 ± 0.1	44.0 ± 3.2
Q62	94.7 ± 11	27.6 ± 3.7	2.3 ± 0.1	48.6 ± 2.6
Q63	457 ± 38	93.4 ± 4.6	5.0 ± 0.3	243 ± 8.1
Q64	59.2 ± 6.2	14.3 ± 0.7	3.4 ± 0.1	84.9 ± 1.7
Tetrofosmin	145 ± 19	7.5 ± 0.8	2.3 ± 0.2	92.0 ± 4.8
Sestamibi	187 ± 12	5.1 ± 0.1	3.9 ± 0.2	179 ± 6.0

*Shown are values from KB-3-1 cells in the absence or presence of high K^+/valinomycin buffer and MDR KB-8-5 cells in the absence or presence of cyclosporin A. Values [fmol/(mg protein·nM_o)] represent the mean ± s.e.m. of four determinations.

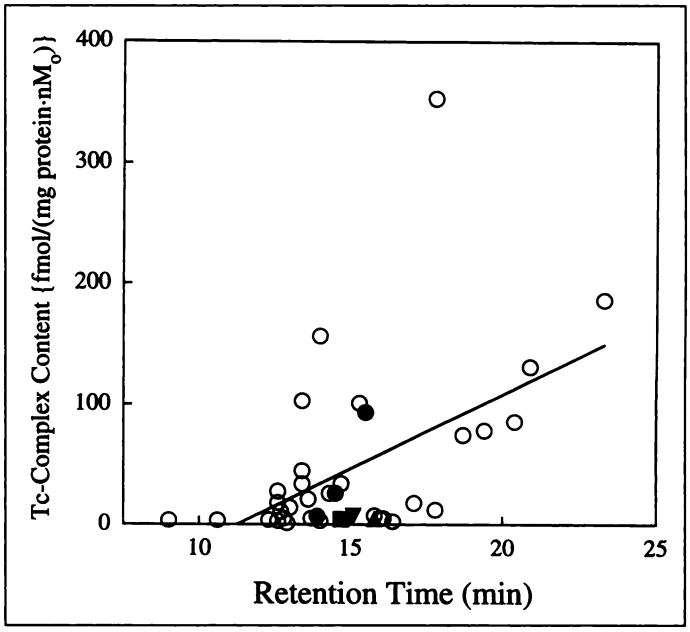

FIGURE 5. Membrane potential-independent accumulation of novel Tc(III)-Q complexes in KB-3-1 cells. Residual cell accumulation of each Tc-Q complex in high K^+/valinomycin buffer (30 min) is plotted as a function of reverse-phase HPLC retention time of each Tc complex (min). Each point represents a different Tc-Q complex (○). The most favorable new agents (Tc-Q57, Tc-Q58 and Tc-Q63; ●), Tc-Q12 (■), ^{99m}Tc-sestamibi (▲) and ^{99m}Tc-tetrofosmin (▼), also are shown for comparison. The solid line represents a linear regression: y = 12.4x −138.9 (r = 0.512, p < 0.005).

lation in the absence of the drug, was a monitor of the MDR modulator-induced reversal. Biochemical and pharmacological considerations would infer that high membrane potential responsiveness, high Pgp distinctions and a high MDR reversal signal would be desirable for a lipophilic cationic *MDR1* Pgp transport substrate. Thus, the MDR SI, a unitless ratio, was defined as the sum of the membrane potential response, the MDR response and the reversal response. The calculated MDR SI for novel Tc-Q complexes and comparative values for ^{99m}Tc-sestamibi, Tc-Q12 and ^{99m}Tc-tetrofosmin also are shown in Figure 7. Tc-Q51, Tc-Q55, Tc-Q57, Tc-Q58 and Tc-Q63, as well as ^{99m}Tc-tetrofosmin, displayed MDR SI values that approximated or exceeded that of ^{99m}Tc-sestamibi. These agents concurrently displayed the highest MDR targeting ratio, with particularly striking transport differences between KB-3-1 and KB-8-5 cells, as well as high reversal in KB-8-5 cells (also see Table 2). There was no correlation between net cell uptake and high MDR SI. For example, whereas the absolute KB-3-1 cell accumulation level for Tc-Q63 was among the highest of

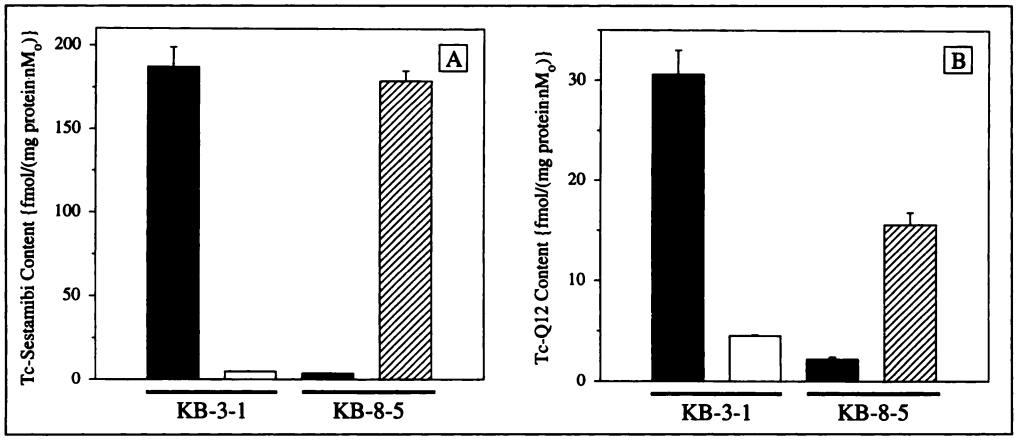

FIGURE 4. Characterization of ^{99m}Tc-sestamibi (A) and Tc-Q12 (B) accumulation in KB-3-1 cells and MDR KB-8-5 cells as indicated. Shown is 30 min net uptake [fmol/(mg protein·nM_o)] in control buffer (solid bar), in 130 m*M* K^+/valinomycin buffer (open bar) and in control buffer containing the MDR modulator cyclosporin A (6 μg/ml; 5 μ*M*) (hatched bars). Each column represents the mean of four determinations; small bars, s.e.m.

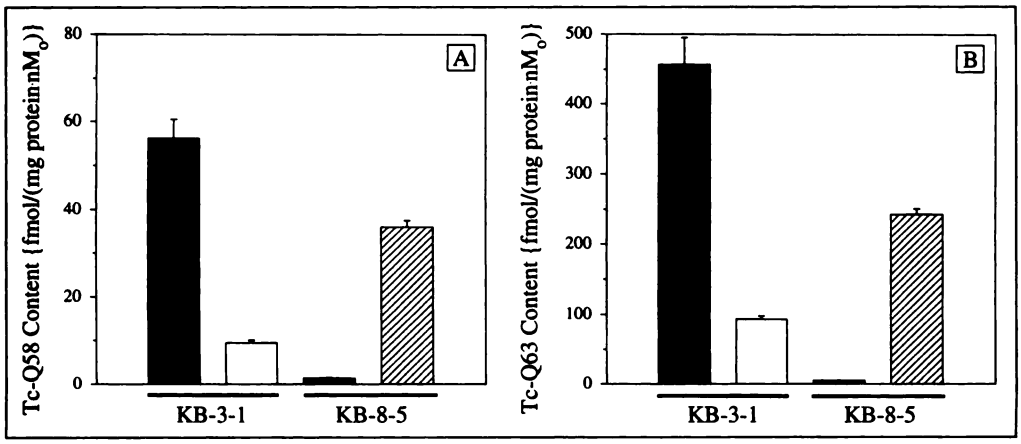

FIGURE 6. Characterization of Tc-Q58 (A) and Tc-Q63 (B) accumulation in KB-3-1 cells and MDR KB-8-5 cells as indicated. Shown is 30 min net uptake [fmol/(mg protein·nM_o)] in control buffer (solid bar), in 130 mM K^+/valinomycin buffer (open bar) and in control buffer containing the MDR modulator cyclosporin A (6 μg/ml; 5 μM) (hatched bars). Each column represents the mean of four determinations; small bars, s.e.m.

this series, other highly favorable complexes, such as Tc-Q58, showed modestly low cell accumulation levels. In addition, further pharmacological specificity for promising complexes was shown in KB-8-5 cells, in which the non-MDR agents methotrexate and cisplatin had no significant effect on Tc-Q58 and Tc-Q63 accumulation (data not shown).

DISCUSSION

The general inorganic chemical characterization of this class of Schiff base mixed ligand Tc(III)-Q complexes has been reported (*23*). These complexes are highly stable in the Tc(III) oxidation state, reducible to Tc(II) only at applied potentials that are not relevant to biological systems (*23,35*) and, thus, have been characterized as nonreducible ^{99m}Tc(III) cations. The class also may offer advantages for *MDR1*-targeted drug discovery and synthesis. For example, because of the symmetry of hexakis Tc(I)-isonitrile complexes, another class of *MDR1*-targeted radiopharmaceuticals, chemically small changes in the substituted isonitrile ligand are multiplied sixfold on formation of the final hexakis-metal complex. It could be argued that more subtle changes may be necessary in the final complex to confer optimal *MDR1* targeting and, indeed, selectively constructing smaller changes into the Schiff base or phosphine ligands of these hetero-complexes is readily accomplished. These agents thus maintain the desired modest lipophilicity and delocalized cationic charge of many other Pgp substrates and modulators while enabling selective exploration of single or paired modified functionalities.

Several agents emerged from our systematic search through portions of the available Tc-Q chemical diversity plane. The most promising agents, based on the optimized MDR SI, were Tc-Q57, Tc-Q58 and Tc-Q63, which met or exceeded the MDR-targeting properties of ^{99m}Tc-sestamibi. Also showing significant overall promise were Tc-Q51 and Tc-Q55; however, data indicated that Tc-Q51 and Tc-Q55 possessed approximately 100% and 14% serum protein binding (Table 1), respectively, thereby eliminating them as candidate agents for applications in vivo. Several additional agents also showed desirable, but somewhat less robust MDR-targeting properties in cell culture, for example, Tc-Q28, Tc-Q40, Tc-Q49, Tc-Q59, Tc-Q61, Tc-Q62 and Tc-Q64.

Several groups have previously performed systematic and statistically significant structure-activity relationships of targeting moieties for compounds in the MDR phenotype. No one element has been shown to be crucial, except that the vast majority of MDR agents possess modest lipophilicity and a cationic charge at neutral pH (*4*). Nonetheless, among a series of reserpine and yohimbine analogs, the presence of pendent benzoyl moieties, in particular those containing trimethoxy substitutions, appeared most effective in enhancing activity (*36*). Similar characteristics were identified with verapamil analogs, including modest lipophilicity, cationic charge and the presence of methoxy functionalities (*4*). In a series of aromatic isonitrile Tc(I) complexes targeting MDR Pgp, methoxy functionalities also conferred Pgp recognition to this class of radiopharmaceuticals (*37*). Indeed, ^{99m}Tc-sestamibi and ^{99m}Tc-tetrofosmin, each validated as *MDR1* Pgp transport substrates, also contain peripheral alkoxy substitutions. Therefore, the finding in this study that those Tc-Q complexes displaying the most robust *MDR1* Pgp transport profiles contained multiple alkoxy substitutions on the Schiff base or phosphine ligands or both, was not without precedent.

Analysis of the quantitative transport data for the promising Tc-Q complexes showed some interesting trends regarding possible biochemical mechanisms of Pgp. Compared to other lipophilic cationic metallopharmaceuticals, such as Tc-isonitriles complexes, the most favorable Tc-Q complexes appeared to uncouple, for the first time, membrane potential responsiveness from *MDR1* Pgp transport. For example, ^{99m}Tc-sestamibi has a well-characterized quantitative membrane potential response revealed by high K^+/valinomycin buffer (*25,32*) that is equal in magnitude to the tracer content differential between the nonexpressing and *MDR1* expressing cells (Table 2). Conversely, in a recent series of more hydrophobic substituted arylisonitrile Tc-complexes, agents concurrently displayed both low membrane potential responsiveness and modest *MDR1* transport recognition (*37*). However, the best of the Tc-Q complexes possess relatively poor membrane potential responsiveness but an *MDR1* Pgp difference signal even greater than ^{99m}Tc-sestamibi. This may imply that the Tc-Q complexes intercalate into lipid compartments or bilayers in a manner that prohibits robust inward translocation in response to imposed transmembrane potentials yet enables enhanced Pgp binding and outward translocation of these substrates by putative intramembranous domains of the transporter (*38*).

CONCLUSION

This study indicates that Tc-Q57, Tc-Q58 and Tc-Q63 are avid transport substrates recognized by the human *MDR1* Pgp, with enhanced in vitro targeting properties relative to Tc-sestamibi. This may enable functional imaging of Pgp in vivo with improved signal-to-noise ratios and tissue contrast. Under identical conditions, ^{99m}Tc-tetrofosmin also is an avid transport substrate. The ability to noninvasively image the Pgp transporter in vivo will provide a significant new tool for understanding MDR in cancer patients. In addition, SPECT imaging of *MDR1* Pgp with a ^{99m}Tc-based tracer may ultimately be used to guide chemotherapeutic protocols, stratify patient response

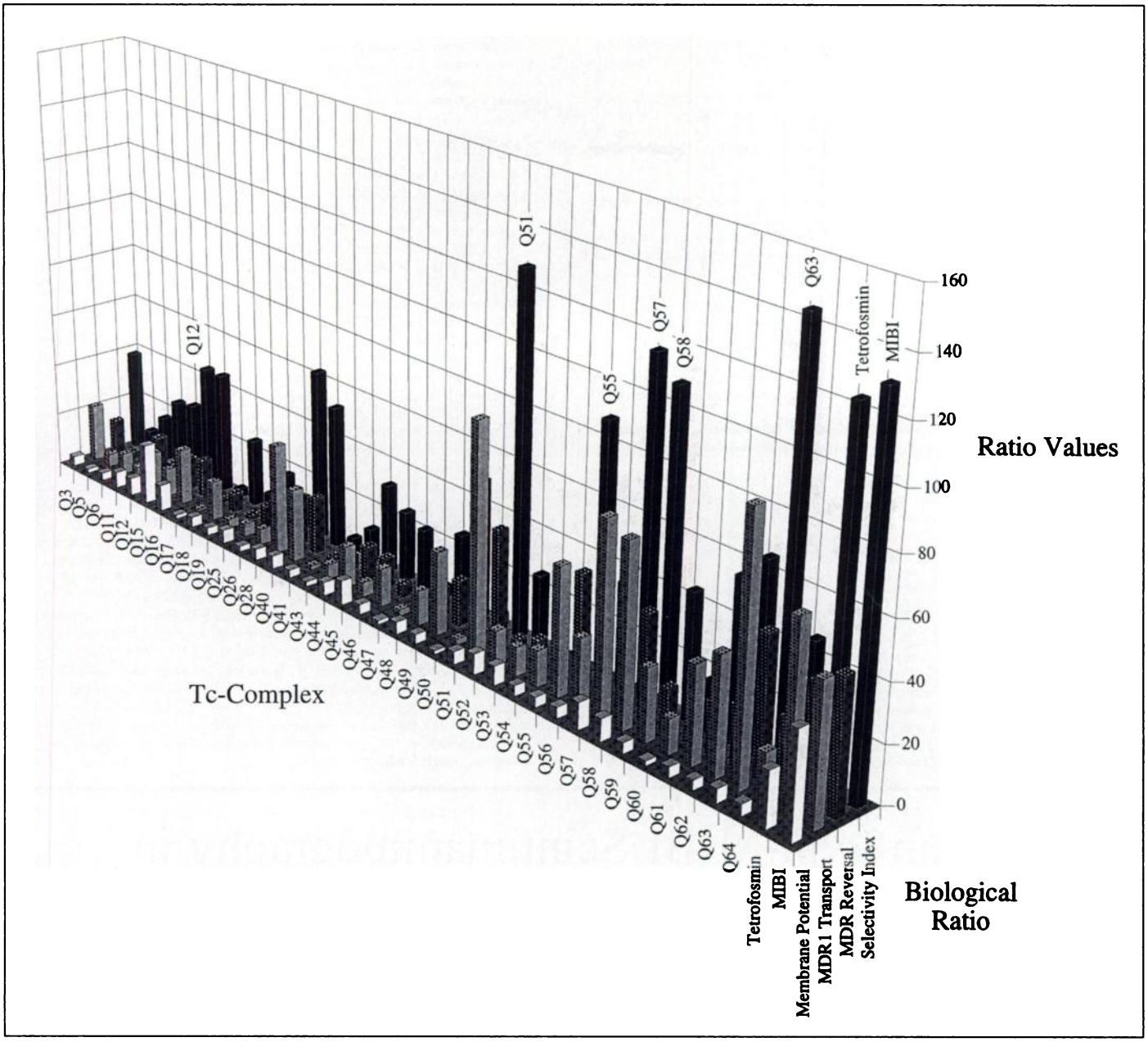

FIGURE 7. Functional ratio values (z-axis) of the novel Tc-Q complexes used to rank biological response properties and *MDR1* Pgp transport targeting. Shown are the membrane potential responsiveness ratios (front row), *MDR1* Pgp-mediated transport ratios (second row), MDR modulator-induced reversal ratios (third row) and the MDR SI (last row) for the novel Tc-Q complexes in comparison to ^{99m}Tc-sestamibi and ^{99m}Tc-tetrofosmin. Each ratio, a unitless value, was calculated as described in the text. Highlighted by identification above the columns are the favorably targeted Tc-Q complexes (Tc-Q57, Tc-Q58 and Tc-Q63) as well as Tc-Q12, ^{99m}Tc-sestamibi and ^{99m}Tc-tetrofosmin for comparison. Excluded from further consideration were Tc-Q51 and Tc-Q55 because of excessive plasma binding.

rates and assist clinical trials or screening of new MDR-reversing agents in patients with cancer.

ACKNOWLEDGMENTS

This work was supported by a research contract from Mallinckrodt Medical, Inc., and by United States Department of Energy Grant ER61885. Gary D. Luker is a recipient of a Society of Nuclear Medicine Mallinckrodt Research Fellowship. David Piwnica-Worms is an Established Investigator of the American Heart Association. We thank Steven Woulfe and Raghavan Rajagopalan for synthesizing various Schiff base and phosphine ligands.

REFERENCES

1. Gottesman MM, Pastan I. Biochemistry of multidrug resistance mediated by the multidrug transporter. *Annu Rev Biochem* 1993;62:385–427.
2. Gros P, Ben Neriah Y, Croop JM, Housman DE. Isolation and expression of a complementary DNA that confers multidrug resistance. *Nature* 1986;323:728–731.
3. Shen DW, Fojo A, Chin JE, et al. Human multidrug-resistant cell lines: increased MDR1 expression can precede gene amplification. *Science* 1986;232:643–645.
4. Ford JM, Hait WN. Pharmacology of drugs that alter multidrug resistance in cancer. *Pharmacol Rev* 1990;42:155–199.
5. Gaveriaux C, Boesch D, Jachez B. PSC 833, a non-immunosuppressive cyclosporin analog, is a very potent multidrug-resistance modifier. *J Cell Pharmacol* 1991;2:225–234.
6. Hyafil F, Vergely C, Du Vignaud P, Grand-Perret T. In vitro and in vivo reversal of multidrug resistance by GF120918, an acridonecarboxamide derivative. *Cancer Res* 1993;53:4595–4602.
7. Cole SPC, Bhardwaj G, Gerlach JH, et al. Overexpression of a transporter gene in a multidrug-resistant human lung cancer cell line. *Science* 1992;258:1650–1654.
8. Baldini N, Scotlandi K, Barbanti-Brodano G, et al. Expression of P-glycoprotein in high-grade osteosarcomas in relation to clinical outcome. *N Engl J Med* 1995;333:1380–1385.
9. Norris M, Bordow S, Marshall G, Haber P, Cohn S, Haber M. Expression of the gene for multidrug-resistance-associated protein and outcome in patients with neuroblastoma. *N Engl J Med* 1996;334:231–238.
10. Wackers FJ, Berman D, Maddahi J, et al. Tc-99m-hexakis 2-methoxy isobutylisoni-

trile: human biodistribution, dosimetry, safety and preliminary comparison to thallium-201 for myocardial perfusion imaging. *J Nucl Med* 1989;30:301–309.
11. Higley B, Smith FW, Smith T, et al. Technetium-99m-1,2-bis[bis(2-ethoxyethyl)phosphino]ethane: human biodistribution, dosimetry and safety of a new myocardial perfusion imaging agent. *J Nucl Med* 1993;34:30–38.
12. Rossetti C, Vanoli G, Paganelli G, et al. Human biodistribution, dosimetry and clinical use of technetium(III)-99m-Q12. *J Nucl Med* 1994;35:1571–1580.
13. Piwnica-Worms D, Chiu ML, Budding M, Kronauge JF, Kramer RA, Croop JM. Functional imaging of multidrug-resistant P-glycoprotein with an organotechnetium complex. *Cancer Res* 1993;53:977–984.
14. Rao VV, Chiu ML, Kronauge JF, Piwnica-Worms D. Expression of recombinant human multidrug resistance P-glycoprotein in insect cells confers decreased accumulation of technetium-99m-sestamibi. *J Nucl Med* 1994;35:510–515.
15. Ballinger J, Hua H, Berry B, Firby P, Boxen I. ^{99m}Tc-sestamibi as an agent for imaging P-glycoprotein-mediated multi-drug resistance: in vitro and in vivo studies in a rat breast tumour cell line and its doxorubicin-resistant variant. *Nucl Med Commun* 1995;16:253–257.
16. Crankshaw CL, Marmion M, Burleigh BD, Deutsch E, Piwnica-Worms D. Non-reducible mixed ligand Tc(III) cations (Q complexes) are recognized as transport substrates by the human multidrug-resistance (MDR) P-glycoprotein [Abstract]. *J Nucl Med* 1995;36:130P.
17. Piwnica-Worms D, Rao V, Kronauge J, Croop J. Characterization of multidrug-resistance P-glycoprotein transport function with an organotechnetium cation. *Biochemistry* 1995;34:12210–12220.
18. Cordobes M, Starzec A, Delmon-Moingeon L, et al. Technetium-99m-sestamibi uptake by human benign and malignant breast tumor cells: correlation with MDR gene expression. *J Nucl Med* 1996;37:286–289.
19. Ballinger JR, Bannerman J, Boxen I, Firby P, Hartman NG, Moore MJ. Technetium-99m-tetrofosmin as a substrate for P-glycoprotein: in vitro studies in multidrug-resistant breast tumor cells. *J Nucl Med* 1996;37:1578–1582.
20. Del Vecchio S, Ciarmiello A, Potena MI, et al. In vivo detection of multidrug-resistant (MDR1) phenotype by technetium-99m sestamibi scan in untreated breast cancer patients. *Eur J Nucl Med* 1997;24:150–159.
21. Luker GD, Fracasso PM, Dobkin J, Piwnica-Worms D. Modulation of the multidrug resistance P-glycoprotein: detection with Tc-99m-sestamibi in vivo. *J Nucl Med* 1997;38:369–372.
22. Deutsch E, Vanderheyden J-L, Gerundini P, et al. Development of nonreducible technetium-99m(III) cations as myocardial perfusion imaging agents: initial experience in humans. *J Nucl Med* 1987;28:1870–1880.
23. Jurisson SS, Dancey K, McPartlin M, Tasker PA, Deutsch E. Synthesis, characterization, and electrochemical properties of technetium complexes containing both tetradentate Schiff base and monodentate tertiary phosphine ligands: single-crystal structure of trans-(N,N′-ethylenebis(acetylacetone iminato))bis(triphenylphosphine)technetium(III) hexafluorophosphate. *Inorg Chem* 1984;23:4743–4749.
24. Woulfe S, Dunn T, Marmion M, MacDonald J, Rogic M, Deutsch E. The synthesis of analogous N_2O_2, N_2OS and diamide dimercapto Schiff base ligands for use in radiopharmaceutical imaging agents [Abstract]. *J Nucl Med* 1991;32:1101.
25. Piwnica-Worms D, Kronauge JF, Chiu ML. Uptake and retention of hexakis (2-methoxy isobutyl isonitrile) technetium(I) in cultured chick myocardial cells: mitochondrial and plasma membrane potential dependence. *Circulation* 1990;82:1826–1838.
26. Sharma V, Crankshaw C, Piwnica-Worms D. Effects of multidrug resistance (*MDR1*) P-glycoprotein expression levels and coordination metal on the cytotoxic potency of multidentate (N_4O_2) ethylenediamine-bis[propyl(R-benzylimino)]metal(III) cations. *J Med Chem* 1996;39:3483–3490.
27. Piwnica-Worms D, Jacob R, Horres CR, Lieberman M. Transmembrane chloride flux in tissue-cultured chick heart cells. *J Gen Physiol* 1983;81:731–748.
28. Lamson ML, Kirscher AS, Hotte CE, Lipsitz EL, Ice RD. Generator-produced ^{99m}Tc-TcO_4^-: carrier free? *J Nucl Med* 1975;16:639–641.
29. Glantz SA. *Primer of biostatistics*, 2nd ed. New York: McGraw-Hill, Inc.; 1987:379.
30. Choi K, Chen CJ, Kriegler M, Roninson IB. An altered pattern of cross-resistance in multidrug-resistant human cells results from spontaneous mutations in the *MDR1* (P-glycoprotein) gene. *Cell* 1988;53:519–529.
31. Chiu ML, Kronauge JF, Piwnica-Worms D. Effect of mitochondrial and plasma membrane potentials on accumulation of hexakis (2-methoxyisobutyl isonitrile) technetium(I) in cultured mouse fibroblasts. *J Nucl Med* 1990;31:1646–1653.
32. Chernoff DM, Strichartz GR, Piwnica-Worms D. Membrane potential determination in large unilamellar vesicles with hexakis(2-methoxyisobutyl isonitrile) technetium(I). *Biochim Biophys Acta* 1993;1147:262–266.
33. Katzenellenbogen JA, Johnson HJJ, Myers HN. Photoaffinity labels for estrogen binding proteins of rat uterus. *Biochemistry* 1973;12:4085–4092.
34. Katzenellenbogen JA. The pharmacology of steroid radiopharmaceuticals: specific and non-specific binding and uptake selectivity. In: Nunn, A., ed. *Radiopharmaceuticals: chemistry and pharmacology*. New York: Marcel Dekker; 1992:297–331.
35. Ichimura A, Heineman WR, Deutsch E. Technetium electrochemistry. 3. Spectroelectrochemical studies on the mixed-ligand technetium(III) complexes trans-$[Tc(PR_2R')_2L]^+$ where L is a tetradentate Schiff base ligand and PR_2R' is a monodentate tertiary phosphine ligand. *Inorg Chem* 1985;24:2134–2139.
36. Pearce HL, Safa AR, Bach NJ, Winter MA, Cirtain MC, Beck WT. Essential features of the P-glycoprotein pharmacophore as defined by a series of reserpine analogs that modulate multidrug resistance. *Proc Natl Acad Sci USA* 1989;86:5128–5132.
37. Herman LW, Sharma V, Kronauge JF, Barbarics E, Herman LA, Piwnica-Worms D. Novel hexakis(areneisonitrile)technetium(I) complexes as radioligands targeted to the multidrug resistance P-glycoprotein. *J Med Chem* 1995;38:2955–2963.
38. van Helvoort A, Smith AJ, Sprong H, et al. *MDR1* P-glycoprotein is a lipid translocase of broad specificity, while *MDR3* P-glycoprotein specifically translocates phosphatidylcholine. *Cell* 1996;87:507–517.

Technetium-99m-MIBI Scintimammography in Palpable and Nonpalpable Breast Lesions

Sergey Mekhmandarov, Judith Sandbank, Maya Cohen, Shlomo Lelcuk and Ernesto Lubin

Departments of Nuclear Medicine, Pathology, Radiology and Surgery, Rabin Medical Center, Beilinson Campus, Petah Tiqva; and Sackler School of Medicine, Tel Aviv University, Tel Aviv, Israel

The aim of this study was to determine the diagnostic accuracy of ^{99m}Tc-MIBI scintimammography in patients with palpable and nonpalpable breast cancer. **Methods:** One hundred and forty patients with a clinically palpable breast mass and/or suspicious mammographic finding had prone scintimammography after the intravenous injection of 740 MBq ^{99m}Tc-MIBI within 5 days before open biopsy or surgery. All patients had mammography within 2 mo before the scintimammography. The mammography was read as probably benign, probably malignant or indeterminate. The scintimammography was read as positive or negative for breast cancer. The scintigraphic studies were correlated with mammographic findings and with histopathology. **Results:** Histopathological studies showed that the mean tumor size for 61 palpable tumors was 2.57 cm with a range of 1–6 cm, and for 24 nonpalpable tumors the mean size was 1.34 cm with a range of 0.5–3 cm. Mammography had an overall sensitivity of 91.58% and a specificity of 42.87%; the sensitivity was 90.16% and 95.45% and specificity was 57.14% and 32.14% for palpable and nonpalpable tumors, respectively. Eight cases were considered indeterminate. Scintimammography was true-positive for 71 breast cancers, true-negative for 47, false-positive for 8 and false-negative for 14. The overall sensitivity was 83.5% and the specificity 85.4%. In the patients with palpable masses, sensitivity was 95.1% and specificity 75%; in those with nonpalpable lesions, sensitivity was only 54.2% and specificity, 93.5%. Among 18 cases of palpable abnormalities with probably benign mammography, six had true-positive scintimammography. Of eight patients with indeterminate mammography, one was true-positive on scintimammography. **Conclusion:** Scintimammography is an accurate and clinically useful tool for evaluating patients with palpable breast abnormalities when mammography is negative and in the cases of indeterminate mammography. A significant improvement in lesion detectability is necessary in nonpalpable breast abnormalities.

Key Words: scintimammography; breast cancer; technetium-99m-MIBI

J Nucl Med 1998; 39:86–91

Breast cancer is the most frequently diagnosed malignancy in Israeli women, accounting for 31% of all female malignancies. Almost 2000 new cases were diagnosed in 1992, and the annual incidence is 80/100,000. In the U.S., the incidence of breast

Received Aug. 29, 1996; revision accepted Apr. 15, 1997.

For correspondence or reprints contact: Sergey Mekhmandarov, MD, Department of Nuclear Medicine, Rabin Medical Center, Beilinson Campus, Petah Tiqva 49100, Israel.